As for the interaction between chains, it can be associated with the hydrogen-bonding networks along the two pathways Cu-N-(H$_3$)-O-Cu with d_{N-O} = 3.048 Å and d_{Cu-Cu} = 5.22 Å, and Cu-N(H$_3$)-Br-Cu with d_{N-Br} = 3.156 Å and d_{Cu-Cu} = 5.22 Å. These pathways are represented in Figure 6. They involve nitrogen, oxygen, or bromine atoms directly bound to copper atoms, on which the spin density is partially delocalized, so that they may efficiently transmit the interaction between metal atoms belonging to different chains and separated by 5.22 Å. Therefore, the interchain interaction is far from being negligible and is actually of the same order of magnitude as the intrachain interaction

through the carboxylate bridge, which explains the high temperature of 3-D antiferromagnetic ordering.

Contribution from the Department of Chemistry, The University, Southampton S09 5NH, U.K., and Daresbury Laboratory, Daresbury, Warrington WA4 4AD, U.K.

Coordination Chemistry of Higher Oxidation States. 19.[†] Synthesis and Properties of Diphosphine and Diarsine Complexes of Iron(IV) and Iron K-Edge EXAFS Data on [Fe(o-C$_6$H$_4$(PMe$_2$)$_2$)$_2$Cl$_2$]$^{n+}$[BF$_4$]$_n$ (n = 0–2)

Stephen K. Harbron,[‡] Simon J. Higgins,[‡] William Levason,*[‡] Martinus C. Feiters,[§] and Andrew T. Steel[§]

Received August 26, 1985

Pure samples of the iron(IV) complexes [Fe(L-L)$_2$X$_2$][BF$_4$]$_2$ (L-L = o-C$_6$H$_4$(PMe$_2$)$_2$, o-C$_6$H$_4$(PMe$_2$)(AsMe$_2$), o-C$_6$H$_4$(AsMe$_2$)$_2$, X = Cl, Br; L-L = Me$_2$PCH$_2$CH$_2$PMe$_2$, X = Cl) have been isolated, and the corresponding complexes [Fe(o-C$_6$F$_4$(PMe$_2$)$_2$)$_2$X$_2$]$^{2+}$ (X = Cl, Br) and [Fe(Me$_2$PCH$_2$CH$_2$PMe$_2$)$_2$Br$_2$]$^{2+}$ have been obtained in solution. Magnetochemical, IR, and electronic spectroscopic data are reported, and the Fe^{II} ↔ Fe^{III} ↔ Fe^{IV} redox potentials have been studied as a function of L-L and X by cyclic voltammetry. Iron K-edge EXAFS data on the title complexes have been analyzed to provide the iron–ligand bond lengths (Å) for [Fe(o-C$_6$H$_4$(PMe$_2$)$_2$)$_2$Cl$_2$]$^{n+}$ (n = 0, Fe–Cl = 2.35, Fe–P = 2.23; n = +1, Fe–P and Fe–Cl = 2.245 (av); n = 2, Fe–Cl = 2.16, Fe–P = 2.33), and the trends in these values are discussed.

Introduction

The chemistry of iron(IV) is not extensive, but this oxidation state has attracted considerable attention due to its occurrence in oxidized iron porphyrins. The formulation of the oxidation products of iron(III) porphyrins has been a controversial topic, but recent investigations have provided good evidence (especially from ^{57}Fe Mössbauer spectroscopy) for both iron(III) porphyrin π-cation radicals[1–3] and iron(IV) porphyrins[4–7] and very recently for a stable iron(IV) π-radical porphyrin.[8] Among the "simple" iron(IV) complexes are the oxometalates Na$_4$FeO$_4$, Ba$_2$FeO$_4$,[9] dithio-[10–12] and diselenocarbamates[13] [Fe(Z$_2$CNR$_2$)$_3$]$^+$ (Z = S, Se), and 1,1-dithiolates [Fe(S$_2$CCR$_2$)$_3$]$^{2-}$.[14] Iron(IV) complexes with neutral ligands are limited to unstable [Fe(o-C$_6$H$_4$-(AsMe$_2$)$_2$)$_2$X$_2$][BF$_4$]$_2$ (X = Cl, Br)[15,16] and [Fe(o-C$_6$H$_4$-(PMe$_2$)$_2$)$_2$Cl$_2$][ReO$_4$]$_2$,[17] and for these the magnetic properties are disputed and no structural data are available.

We have recently shown[18,19] that structural data can be obtained for similarly unstable nickel(IV) diphosphines by metal K-edge EXAFS, and here we report a similar study of the iron(IV) complexes. A preliminary account of this work has appeared.[20]

Results

The iron(IV) complexes [Fe(L-L)$_2$X$_2$][BF$_4$]$_2$ (L-L = o-C$_6$H$_4$(PMe$_2$)$_2$, o-C$_6$H$_4$(AsMe$_2$)$_2$, o-C$_6$H$_4$(PMe$_2$)(AsMe$_2$); X = Cl, Br) (Table I) were obtained by nitric acid oxidation of the iron(III) analogues, followed by precipitation with HBF$_4$. Since purity is often markedly dependent upon the counterion (cf. ref 19), other ions including ClO$_4^-$, ReO$_4^-$, PF$_6^-$, and CF$_3$SO$_3^-$ were considered. (The isolation of [FeCl$_4$]$^-$ salts has been reported,[15] but the presence of a second iron center makes them unsuitable for magnetochemical and EXAFS studies.) The perchlorates are highly explosive,[15] the perrhenates are prone to introduce nit-

rogenous impurities, and while PF$_6^-$ readily gave precipitates of the iron(IV) complexes, these had poor analyses and the IR spectra showed other fluorophosphate ions to be present (mainly PO$_2$F$_2^-$). Trifluoromethanesulfonic acid did not precipitate the complexes from solution, and hence the BF$_4^-$ salts were used in this study. Although these are reportedly[16] hygroscopic, we found that *thoroughly dried* pure samples absorbed water only slowly. The syntheses are described in the Experimental Section, purity being

(1) Boersma, A. D.; Goff, H. M. *Inorg. Chem.* **1984**, *23*, 1671 and references therein.
(2) Phillippi, M. A.; Goff, H. M. *J. Am. Chem. Soc.* **1982**, *104*, 6026.
(3) Shimomura, E. T.; Phillippi, M. A.; Goff, H. M.; Scholz, W. F.; Reed, C. A. *J. Am. Chem. Soc.* **1981**, *103*, 6778.
(4) Kadish, K. M.; Rhodes, R. K.; Bottomley, L. A.; Goff, H. M. *Inorg. Chem.* **1981**, *20*, 3195.
(5) English, D. R.; Hendrickson, D. N.; Suslick, K. S. *Inorg. Chem.* **1983**, *22*, 367.
(6) Hiller, W.; Strahle, J.; Datz, A.; Hanack, M.; Hatfield, W. E.; ter Haar, L. M.; Gutlich, P. *J. Am. Chem. Soc.* **1984**, *106*, 329.
(7) Grove, J. T.; Quinn, R.; McMurray, T. J.; Nakamura, M.; Lang, G.; Boso, B. *J. Am. Chem. Soc.* **1985**, *107*, 354.
(8) English, D. R.; Hendrickson, D. N.; Suslick, K. S. *Inorg. Chem.* **1985**, *24*, 123.
(9) Scholder, R. *Z. Elektrochem.* **1952**, *56*, 879. Scholder, R.; Bunsen, H. V.; Zeiss, W. *Z. Anorg. Allg. Chem.* **1956**, *283*, 330.
(10) Pasek, E. A.; Straub, D. K. *Inorg. Chem.* **1972**, *11*, 259.
(11) Chant, R.; Hendrickson, A. R.; Martin, R. L.; Rohde, N. M. *Inorg. Chem.* **1975**, *14*, 1814.
(12) Martin, R. L.; Rohde, N. M.; Robertson, G. B.; Taylor, D. *J. Am. Chem. Soc.* **1974**, *96*, 3647.
(13) Deplano, P.; Trogu, E. F.; Bigoli, F.; Laporate, E.; Pellighelli, M. A.; Perry, D. L.; Saxon, R. J.; Wilson, L. J. *J. Chem. Soc., Dalton Trans.* **1983**, 25.
(14) Hollander, F. J.; Pedelty, R.; Coucouvanis, D. *J. Am. Chem. Soc.* **1974**, *96*, 4032.
(15) Nyholm, R. S.; Parish, R. V. *Chem. Ind. (London)* **1956**, 470.
(16) Hazeldean, G. S. F.; Nyholm, R. S.; Parish, R. V. *J. Chem. Soc. A* **1966**, 162.
(17) Warren, L. F.; Bennett, M. A. *Inorg. Chem.* **1976**, *15*, 3126.
(18) Steel, A. T.; Feiters, M. C.; Garner, C. D.; Hasnain, S. S.; Higgins, S. J.; Levason, W. *J. Chem. Soc., Chem. Commun.* **1985**, 484.
(19) Higgins, S. J.; Levason, W.; Feiters, M. C.; Steel, A. T. *J. Chem. Soc., Dalton Trans.* **1986**, 317.
(20) Harbron, S. K.; Higgins, S. J.; Levason, W.; Feiters, M. C.; Steel, A. T.; Garner, C. D.; Hasnain, S. S. *J. Am. Chem. Soc.* **1986**, *108*, 526.

† Part 18: Hope, E. G.; Levason, W.; Webster, M.; Murray, S. G. *J. Chem. Soc., Dalton Trans.*, in press.
‡ The University, Southampton.
§ Daresbury Laboratory.

Table I. Analytical and Physical Data

complex	color	% C^a	% H^a	% X^{ab}	μ_{eff}^c/μ_B	$\nu(FeX)/cm^{-1}$
[Fe(o-C$_6$H$_4$(PMe$_2$)$_2$)$_2$Cl$_2$][BF$_4$]$_2$	purple	35.0 (34.5)	4.7 (4.6)	10.0 (10.2)	3.01	384 (378)
[Fe(o-C$_6$H$_4$(PMe$_2$)$_2$)$_2$Br$_2$][BF$_4$]$_2$	dark green	30.3 (30.6)	4.2 (4.1)	20.4 (20.4)	2.71	303 (298)
[Fe(o-C$_6$H$_4$(PMe$_2$)(AsMe$_2$))$_2$Cl$_2$][BF$_4$]$_2$	green-black	30.3 (30.6)	4.1 (4.1)	9.0 (9.5)	3.22	390 (376)
[Fe(o-C$_6$H$_4$(PMe$_2$)(AsMe$_2$))$_2$Br$_2$][BF$_4$]$_2$	dark green	26.9 (27.5)	3.9 (3.7)	18.4 (18.3)	3.27	294 (290)
[Fe(o-C$_6$H$_4$(AsMe$_2$)$_2$)$_2$Cl$_2$][BF$_4$]$_2$	green-black	27.6 (27.5)	3.8 (3.7)		3.05	390 (374)
[Fe(o-C$_6$H$_4$(AsMe$_2$)$_2$)$_2$Br$_2$][BF$_4$]$_2$	dark green	24.7 (25.0)	3.4 (3.4)	17.0 (16.6)	2.84	317 (303)
[Fe(Me$_2$PCH$_2$CH$_2$PMe$_2$)$_2$Cl$_2$][BF$_4$]$_2$	purple-black	24.3 (23.9)	5.6 (5.3)			386 (371)

^{a}Calculated values in parenthesis. ^{b}X = halogen. ^{c}Gouy method ca. ±0.1. ^{d}Values for Fe(III) analogue in parentheses.

judged both by analysis (including absence of nitrogen) and by the absence of "extra" vibrations in the IR spectra due to NO$^+$ or NO$_3^-$. Nitric acid oxidation produced [Fe-(Me$_2$PCH$_2$CH$_2$PMe$_2$)$_2$X$_2$][BF$_4$]$_2$ in solution, but these were highly soluble and solids could not be isolated. Pure [Fe-(Me$_2$PCH$_2$CH$_2$PMe$_2$)$_2$Cl$_2$][BF$_4$]$_2$ was obtained by chlorine oxidation of the iron(III) complex in CF$_3$CO$_2$H solution, followed by addition of HBF$_4$, and removal of most of the solvent in vacuo. In contrast, the [Fe(o-C$_6$F$_4$(PMe$_2$)$_2$)$_2$X$_2$][BF$_4$] complexes were only slightly soluble in concentrated nitric acid, and although the iron(IV) complexes were formed in solution (electronic spectral evidence; Table II), precipitation from these dilute solutions resulted mainly in recovery of the iron(III) complex.

Attempts to oxidize iron(II) or iron(III) complexes of o-C$_6$H$_4$(PMe$_2$)(SbMe$_2$), o-C$_6$H$_4$(PPh$_2$)$_2$, o-C$_6$H$_4$(PMe$_2$)(SMe), or Ph$_2$PCH$_2$CH$_2$PPh$_2$ with HNO$_3$ resulted in decomposition. Halogens or nitric acid also failed to oxidize [Fe(L'-L')$_3$]X$_2$ or [Fe(L'-L')$_2$X$_2$] (L'-L' = 2,2'-bipyridyl or 1,10-phenanthroline) to iron(IV). It is significant that although [Fe(L'-L')$_3$]$^{4+}$ ions have been prepared electrochemically in liquid sulfur dioxide,[21,22] the electron removed from [Fe(L-L)$_3$]$^{3+}$ comes from a ligand orbital. In view of the preparation of [Fe^{IV}(S$_2$CNR$_2$)$_3$]$^+$ by BF$_3$-air oxidation of the iron(III) complexes,[10] we also examined the effect of BF$_3$ on [Fe(diphos)$_2$X$_2$]$^+$ (diphos = o-C$_6$H$_4$(PPh$_2$)$_2$, Ph$_2$PCHCHPPh$_2$) in toluene or CH$_2$Cl$_2$, but although dark solids were produced, these reverted to the green iron(III) complexes on drying.

Properties. The iron(IV) complexes are deep purple to green-black powders that can be stored at −20 °C in the dark for a few days but decompose in a few hours at room temperature. They are insoluble in freons and chlorocarbons and decompose rapidly in most other organic solvents. Anhydrous trifluoroacetic acid is the only solvent in which decomposition is slow enough to allow spectroscopic studies.

The magnetic moments of [Fe(o-C$_6$H$_4$(AsMe$_2$)$_2$)$_2$X$_2$][BF$_4$]$_2$ were originally reported[16] as 2.76 μ_B (Cl) and 3.17 μ_B (Br), but a more recent study[17] reported a value of 3.38 μ_B for the chloride and 3.65 μ_B for [Fe(o-C$_6$H$_4$(PMe$_2$)$_2$)$_2$Cl$_2$][ReO$_4$]$_2$, and it was proposed that lower moments were due to contamination with the Fe(III) analogues. Theory[23] suggests a low-spin d^4 ion in a *regular* octahedral environment should have $\mu_{eff} \approx 3.6$ μ_B, which will be reduced due to partial quenching of the orbital moment as the symmetry is lowered. Our values for the six Fe(IV) complexes (Table I) lie in the range ca. 2.7–3.3 μ_B, essentially in agreement with the results of Hazeldean et al.[16] (In view of the inherent instability of these complexes and of the experimental difficulty of preparing pure samples in sufficient quantity for Gouy measurements, realistic error limits would be ±0.1–0.2 μ_B.) In view of the results from a ^{57}Fe Mössbauer study[24] of the iron(IV) diarsine complex that showed a strong axial compression of the ligand field with the (d$_{xy}$)^2(d$_{xz}$)^1(d$_{yz}$)^1 configuration and a d$_{xy}$–d$_{xz}$, d$_{yz}$ separation of ca. 3000 cm^{-1}, the lower magnetic moments appear reasonable. It is notable that the isoelectronic complexes
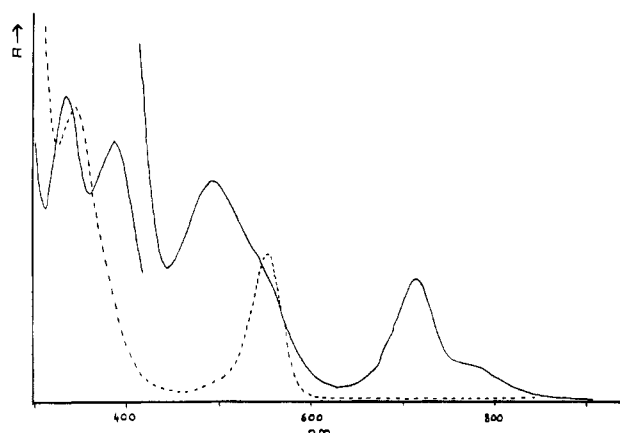

Figure 1. UV–visible spectra of [Fe(o-C$_6$F$_4$(PMe$_2$)$_2$)$_2$Cl$_2$]$^{2+}$ (solid line) and [Fe(o-C$_6$F$_4$(PMe$_2$)$_2$)$_2$Cl$_2$]$^+$ (broken line) in trifluoroacetic acid solution.
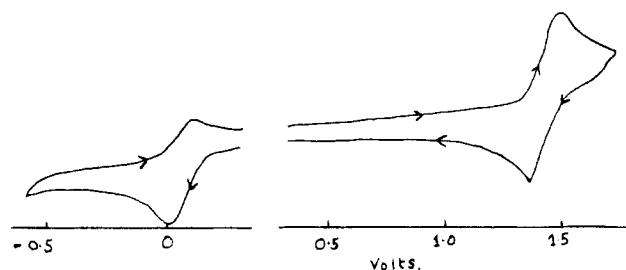
Figure 2. Cyclic voltammogram of [Fe(o-C$_6$H$_4$(PMe$_2$)(AsMe$_2$))$_2$Cl$_2$]$^+$ in acetonitrile with [n-Bu$_4$N][BF$_4$] as supporting electrolyte.

[Cr(o-C$_6$H$_4$(AsMe$_2$)$_2$)$_2$X$_2$]^{25} and [Mn(o-C$_6$H$_4$(PMe$_2$)$_2$)$_2$Cl$_2$]-[PF$_6$]^{17} have μ_{eff} values of 2.8–3.1 μ_B while even the [Fe-(S$_2$CNR$_2$)$_3$]$^+$ compounds, which have a very distorted octahedral geometry, have μ_{eff} lowered to ca. 3.0–3.3 μ_B.[10]

The electronic spectra of the iron(IV) complexes and the iron(III) precursors are given in Table II, and typical examples are illustrated in Figure 1. The Fe(IV) spectra were recorded in trifluoroacetic acid solution, and repetitive scanning revealed decomposition to be relatively slow. The spectra differ significantly from those in ref 16, measured in nitromethane, in which decomposition is much more rapid and in which large amounts of iron(III) appear to be present. Diffuse reflectance spectra of the iron(IV) complexes were similar in profile but less well-defined. Zink et al.[26] proposed an assignment for the spectra of the iron(III) compounds [Fe(o-C$_6$H$_4$(AsMe$_2$)$_2$)$_2$X$_2$]$^+$, the three main bands being ascribed to (As, X) → Fe charge transfer (mainly σ(As) → Fe with some mixing in of halide character[26]). For a low-spin d^5 complex in D_{2h} symmetry the ground state is (d$_{xy}$)^2(d$_{xz}$, d$_{yz}$)^3(d$_{z^2}$)^0(d$_{x^2-y^2}$)^0, and the three main CT bands were thus assigned respectively as (As, X) → Fe$_{d_{xz},d_{yz}}$, → Fe$_{d_{z^2}}$, and → Fe$_{d_{x^2-y^2}}$. The main absorptions in the spectra of the other Fe(III) complexes (Table II) can be assigned in a similar manner. The Fe(IV) complexes show four major absorptions at ca. 12 000–14 000, ca.

(21) Gaudiello, J. G.; Bradley, P. G.; Norton, K. A.; Woodruff, W. H.; Bard, A. J. *Inorg. Chem.* **1984**, *23*, 3.

(22) Gaudiello, J. G.; Sharp, P. R.; Bard, A. J. *J. Am. Chem. Soc.* **1982**, *104*, 6373.

(23) Figgis, B. N.; Lewis, J. *Prog. Inorg. Chem.* **1964**, *6*, 37.

(24) Paez, E. A.; Weaver, D. L.; Ousterhuis, W. T. *J. Chem. Phys.* **1972**, *57*, 3709.

(25) Mani, F.; Stoppioni, P.; Sacconi, L. *J. Chem. Soc., Dalton Trans.* **1975**, 461.

(26) Zink, J. I.; Liu, P-H.; Ansfield, B. *Inorg. Chem.* **1979**, *18*, 1013.

Table II. Electronic Spectroscopic Data

	$E_{max}/10^3$ cm⁻¹ (ϵ_{mol}/dm³ mol⁻¹ cm⁻¹)	
	Fe(III) complex (n = 1)[a]	Fe(IV) complex (n = 2)[b]
$[Fe(o\text{-}C_6H_4(PMe_2)_2)_2Cl_2][BF_4]_n$	17.9 (1980), 20.2 (sh) (190), 28.6 (4370), 33.1 (sh) (10000)	12.7 (sh) (700), 13.8 (1640), 20.0 (3480), 26.1 (9380), 29.9 (12700)
$[Fe(o\text{-}C_6H_4(PMe_2)_2)_2Br_2][BF_4]_n$	16.3 (3320), 18.5 (sh) (270), 25.8 (2230), 34.7 (12900)	11.9 (700), 12.8 (1980), 17.1 (sh) (850), 18.9 (1570), 26.0 (sh) (5290), 28.1 (6520)
$[Fe(o\text{-}C_6H_4(PMe_2)(AsMe_2))_2Cl_2][BF_4]_n$	18.1 (1530), 27.7 (4800), 33.3 (11400)	12.5 (sh) (1180), 13.5 (2770), 18.5 (7830), 24.2 (20500), 28.6 (22800)
$[Fe(o\text{-}C_6H_4(PMe_2)(AsMe_2))_2Br_2][BF_4]_n$	16.6 (3200), 18.2 (sh) (550), 25.0 (2740), 32.5 (10000)	11.8 (530), 12.7 (1570), 16.7 (sh) (1450), 17.7 (1710), 23.5 (5170), 25.5 (5080), 26.5 (5070)
$[Fe(o\text{-}C_6H_4(AsMe_2)_2)_2Cl_2][BF_4]_n$	18.1 (1710), 19.8 (sh) (300), 27.3 (6370), 31.7 (12800)	12.5 (sh) (510), 13.5 (1150), 18.2 (3650), 23.6 (10600), 28.0 (9100)
$[Fe(o\text{-}C_6H_4(AsMe_2)_2)_2Br_2][BF_4]_n$	16.6 (2180), 24.6 (2800), 30.9 (7600)	11.8 (940), 12.6 (2740), 17.4 (3340), 23.0 (10200), 25.1 (8670), 26.5 (8620)
$[Fe(Me_2PCH_2CH_2PMe_2)_2Cl_2][BF_4]_n$	18.1 (1720), 19.6 (sh) (480), 27.9 (4080), 35.7 (21200)	12.7 (sh) (650), 13.4 (1080), 18.9 (3600), 25.9 (8100), 29.2 (14500)
$[Fe(Me_2PCH_2CH_2PMe_2)_2Br_2][BF_4]_n$	16.6 (2780), 18.1 (580), 25.4 (1090), 35.0 (13200)	12.0 (sh), 12.7, 18.0, 25.5 (sh), 27.7[c]
$[Fe(o\text{-}C_6F_4(PMe_2)_2)_2Cl_2][BF_4]_n$	18.2 (2150), 26.9 (sh), (780), 29.2 (4400)	13.0 (sh), 14.0, 18.3 (sh), 20.3, 25.9, 29.8[c]
$[Fe(o\text{-}C_6F_4(PMe_2)_2)_2Br_2][BF_4]_n$	16.1 (3200), 17.7 (sh) (270), 25.6 (1900), 34.3 (10100)	11.9 (sh), 12.9, 19.0, 25.1 (sh), 26.5 (sh), 27.7[c]

[a] In MeCN solution. [b] CF_3CO_2H solution—extinction coefficients are approximate in view of the instability in solution. [c] Generated in situ. All spectra were recorded over the range ~300–900 nm.

Table III. Electrochemical Data

starting material	Fe^{II} ← Fe^{III}/mV[a]	ΔP/mV	IP$_{ox}$/IP$_{red}$	Fe^{III} ↔ Fe^{IV}/mV[a]	ΔP/mV	IP$_{ox}$/IP$_{red}$
$[Fe(o\text{-}C_6H_4(PMe_2)_2)_2Cl_2][BF_4]$	+45	70	1.07	+1430	90	1.05
$[Fe(o\text{-}C_6H_4(PMe_2)_2)_2Br_2][BF_4]$	+190	140	0.71	+1370	90	
$[Fe(o\text{-}C_6H_4(PMe_2)(AsMe_2))_2Cl_2][BF_4]$	+50	100	0.47	+1420	120	0.94
$[Fe(o\text{-}C_6H_4(AsMe_2)_2)_2Cl_2][BF_4]$	not obsd			+1440	70	0.88
$[Fe(o\text{-}C_6F_4(PMe_2)_2)_2Cl_2][BF_4]$	+345	90	0.95	+1690	85	1.08
$[Fe(o\text{-}C_6H_4(PPh_2)_2)_2Cl_2]$[b]	+110	100	1.00	+1010	irreversible	
$[Fe(Me_2PCH_2CH_2PMe_2)_2Cl_2][BF_4]$	−175	irreversible		+1220	80	1.09
$[Fe(Me_2PCH_2CH_2PMe_2)_2Br_2][BF_4]$	−60	irreversible		+1180	70	1.03

[a] In MeCN vs. standard calomel electrode, with [N-n-Bu₄][BF₄] as supporting electrolyte. Scans: 200 mV/min. [b] In CH₂Cl₂ vs. standard calomel electrode, with [N-n-Bu₄][BF₄] as supporting electrolyte. Scans: 200 mV/min.

17000–20000, ca. 23000–26000, and ca. 26000–30000 cm⁻¹, the first three of which can be assigned as (L) → Fe$_{d_{xz},d_{yz}}$, → Fe$_{d_{z^2}}$, and → Fe$_{d_{x^2-y^2}}$ charge transfer. The bathochromic shift is expected as the oxidation state of the metal increases, but it is noticeable that while the second and third bands shift to lower energy by ca. 8000 cm⁻¹, the first shifts by only ca. 4000 cm⁻¹. This indicates that the d$_{xz}$, d$_{yz}$ – d$_{z^2}$ separation is smaller in the Fe(IV) complexes, which could result from strong Cl π-d$_{xz}$, d$_{yz}$ interaction, and this correlated well with the short Fe^{IV}–Cl bond length established by the EXAFS study of $[Fe(o\text{-}C_6H_4(PMe_2)_2)_2Cl_2][BF_4]_2$ (below). Assignment of the weaker bands in the spectra of the iron(IV) complexes is less clear. We do not think these are due to decomposition products, since in general they do not correspond with bands found in the iron(III) complexes and, secondly, repetitive scanning shows that they decrease in parallel with the stronger absorptions. It is possible that these are d–d transitions. Few low-spin d⁴ complexes are known for the 3d elements, and their spectra have not been examined in detail,[27] but the energies of these weaker transitions seem not unreasonable for d–d bands utilizing one-electron d-orbital energies determined from the CT transitions (cf. ref 26).

$[Fe(L-L)_2X_2]BF_4$ underwent reversible 1e electrochemical oxidations in MeCN solution (Table III, Figure 2) at highly positive potentials, which differed little whether X = Cl or Br. The redox potentials varied very little with ligand among the $o\text{-}C_6H_4(PMe_2)_2$, $o\text{-}C_6H_4(PMe_2)(AsMe_2)$, and $o\text{-}C_6H_4(AsMe_2)_2$ complexes, suggesting that Fe(IV) is equally stabilized by phosphorus or arsenic. The $[Fe(o\text{-}C_6F_4(PMe_2)_2)_2Cl_2]^+$ redox potential was higher, correlating with our failure to isolate the Fe(IV) complex, and that of $[Fe(Me_2PCH_2CH_2PMe_2)_2Cl_2]^+$ rather lower, reflecting the relative donor power of the two di-

phosphines to high-valent metals.[19] The Fe(III) complexes also underwent 1e reductions to Fe(II) complexes, but depending upon the ligand these varied from reversible to quasi-reversible to irreversible. The reasons for this behavior are unclear, although in at least one case, coating of the electrode with the Fe(II) complex appeared to be involved. One phenyldiphosphine complex $[Fe(o\text{-}C_6H_4(PPh_2)_2)_2Cl_2]$ was examined, and although this underwent reversible oxidation to Fe(III), only one further completely irreversible oxidation wave was found at higher potential, and there was no evidence for *reversible* oxidation to Fe(IV).

EXAFS. The instability of even the most robust of the Fe(IV) diphosphine complexes in solution precluded attempts to obtain single crystals for an X-ray study. However, it was possible to obtain Fe–P and Fe–X bond lengths via iron K-edge EXAFS.[20] Data were recorded for the three title complexes (Figure 3), which not only provided the bond lengths for the Fe(IV) complex (n = 2), but placed the changes in Fe–Cl and Fe–P bond lengths in context as the metal's formal oxidation state varied Fe(II)–Fe(III)–Fe(IV).

EXAFS measurements were recorded at the Fe K-edge in the transmission mode at the Daresbury Synchrotron Radiation Source as described elsewhere.[19,20] Data were collected at room temperature (293 K) on undiluted samples that were held between strips of sellotape using an aluminum spacer (0.5 mm thick).

The pre-edge background was removed from each spectrum by fitting the pre-edge region to a second-order polynomial and subtracting this from the entire spectrum. The post-edge background was obtained by using two cubic polynomials with a smooth knot (i.e. the same first derivative at a selected point) approximately 200–300 eV above the edge.[28,29] The resulting background-subtracted data were used in the subsequent curve fitting

(27) Lever, A. B. P. *Inorganic Electronic Spectroscopy*; 2nd ed.; Elsevier: Amsterdam, 1984.

(28) EXBACK1 program.

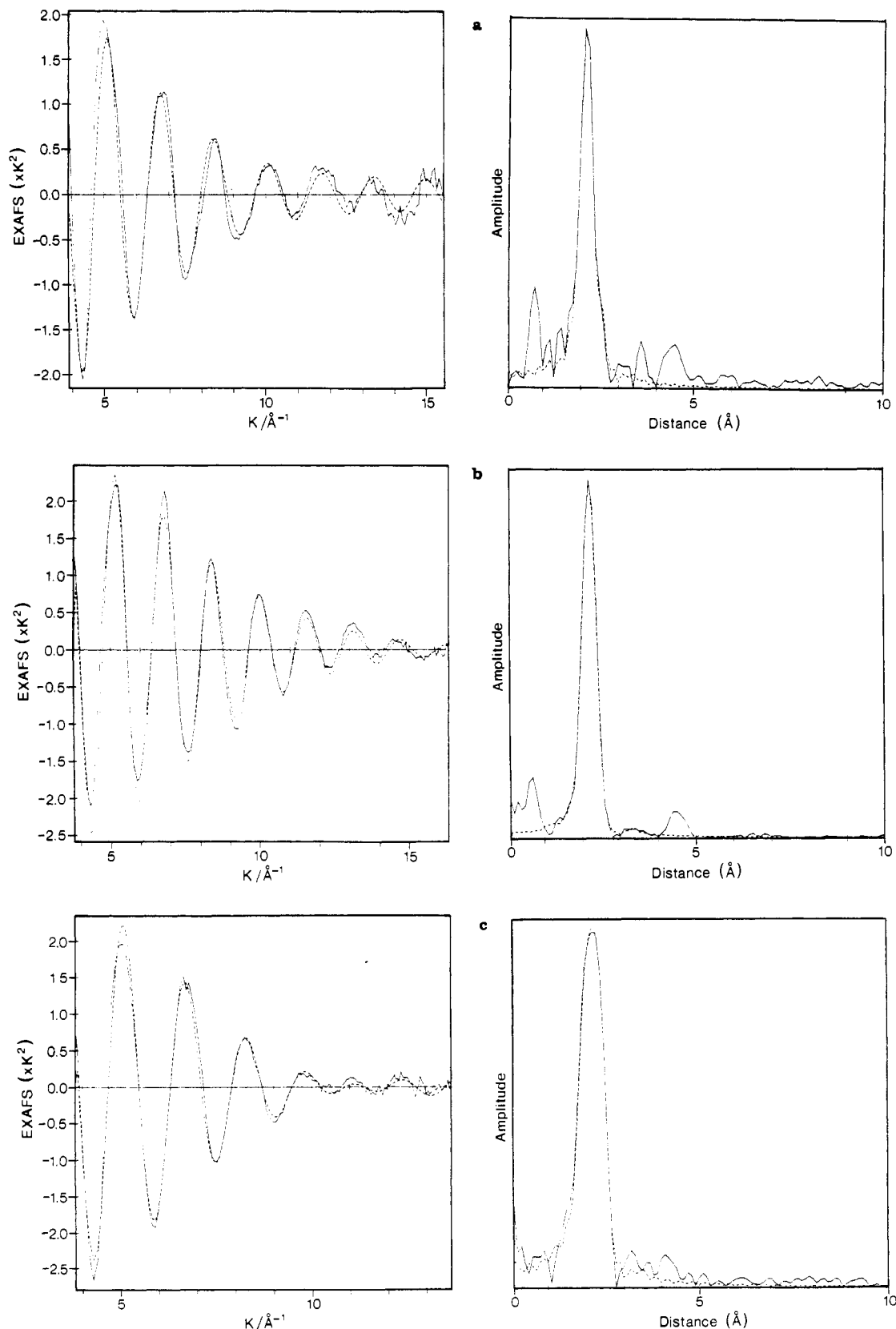(29) MUFPOT, EXCURVE, and EXBACK1 programs available from the SRS program library.

Figure 3. (Background-subtracted) EXAFS and their Fourier transforms of the title complexes (solid line, experimental data; broken line, calculated). No smoothing of Fourier-filtering techniques have been applied to the data: (a) [Fe(o-C$_6$H$_4$(PMe$_2$)$_2$)$_2$Cl$_2$]; (b) [Fe(o-C$_6$H$_4$(PMe$_2$)$_2$)$_2$Cl$_2$][BF$_4$]; (c) [Fe(o-C$_6$H$_4$(PMe$_2$)$_2$)$_2$Cl$_2$][BF$_4$]$_2$.

without smoothing or Fourier filtering.

Phase shifts were calculated by ab initio methods described previously,[30] using the MUFPOT program.[29] The reliability of these

were tested by fitting the EXAFS of [FeCl$_4$]$^-$ and the two diphosphine complexes (*n* = 0, 1). Curve-fitting procedures for simulating the EXAFS are based on the curved-wave theory[31] for EXAFS and are contained in the EXCURVE program.[29,32]

(30) Perutz, M. F.; Hasnain, S. S.; Duke, P. J.; Sessler, J. L.; Hahn, J. E. *Nature (London)* **1982**, *295*, 535.

(31) Lee, P. A.; Pendry, J. B. *Phys. Rev. B: Solid State* **1975**, *11*, 2975.

Table IV. Structural Data

complex	Fe–Cl^a/Å	Fe–P/Å	$2\sigma^{2b}$/Å^2	E°/eV	FI^c/K^2	technique	ref
[Ph$_4$P][FeCl$_4$]	2.19		0.005	22.8	0.14	EXAFS	d
[Ph$_4$As][FeCl$_4$]	2.181 (1)					X-ray	e
[Fe(o-C$_6$H$_4$(PMe$_2$)$_2$)$_2$Cl$_2$]	2.35	2.23	0.007, 0.006	21.7	0.38	EXAFS	d
[Fe(Me$_2$PCH$_2$CH$_2$PMe$_2$)$_2$Cl$_2$]	2.352 (1)	2.241 (1), 2.230 (1)				X-ray	f
[Fe(o-C$_6$H$_4$(PMe$_2$)$_2$)$_2$Cl$_2$][BF$_4$]	2.245	2.245	0.010, 0.010	24.4	0.24	EXAFS	d
[Fe(o-C$_6$F$_4$(PMe$_2$)$_2$)$_2$Cl$_2$][BF$_4$]	2.234 (1)	2.292 (1), 2.295 (1)				X-ray	g
[Fe(o-C$_6$H$_4$(PMe$_2$)$_2$)$_2$Cl$_2$][BF$_4$]$_2$	2.16	2.33	0.007, 0.010	23.1	0.10	EXAFS	d
[Mn(o-C$_6$H$_4$(PMe$_2$)$_2$)$_2$Cl$_2$][ClO$_4$]	2.239 (2)^i	2.344 (av)^i				X-ray	h
[Mn(o-C$_6$H$_4$(PMe$_2$)$_2$)$_2$Cl$_2$][H(NO$_3$)$_2$]$_2$	2.195 (1)^i	2.428 (av)^i				X-ray	h

^{a} With current data analysis programs the errors in the EXAFS bond lengths are ±0.01–0.02 Å. These arise from errors associated with the calculated phase shifts, and the number quoted comes mainly from previous experience of such. ^{b} Debye–Waller factor. ^{c} Analysis involved the least-squares minimization of the function $\sum_i k^2(\chi_i^T - \chi_i^E)^2$. ^{d} This work. ^{e} Reference 29. ^{f} Reference 30. ^{g} Reference 31. ^{h} Reference 17. ^{i} Mn–Cl; Mn–P.

Good agreement of the Fe–Cl bond length as determined by EXAFS with the crystallographic data[33] was achieved for [FeCl$_4$]$^-$ (Table IV). For the diphosphines the coordination number and donor-atom arrangement were fixed as trans six coordinate (P$_4$Cl$_2$), which removes uncertainty in the data treatment due to the strong correlation between the coordination number and the Debye–Waller terms. The similar back-scatterings of phosphorus and chlorine could make this correlation a particular problem in these systems.

For [Fe(o-C$_6$H$_4$(PMe$_2$)$_2$)$_2$Cl$_2$] the Fe–P and Fe–Cl bond lengths are in good agreement with those obtained[34] by X-ray crystallography for the related complex [Fe(Me$_2$PCH$_2$CH$_2$PMe$_2$)$_2$Cl$_2$]. In the case of [Fe(o-C$_6$H$_4$(PMe$_2$)$_2$)$_2$Cl$_2$][BF$_4$] the EXAFS analysis could not distinguish separate Fe–P and Fe–Cl distances due to the very similar back-scatterings of chlorine and phosphorus, and an average value of 2.245 Å is quoted in Table III. The Fe^{III}–P and Fe^{III}–Cl bond lengths are expected to be very similar, and this is supported by the X-ray data[35] on [Fe(o-C$_6$F$_4$-(PMe$_2$)$_2$)$_2$Cl$_2$][BF$_4$]. It should be noted however that the average of the Fe–P and Fe–Cl bond lengths in the latter is 0.03 Å longer than that determined by EXAFS for [Fe(o-C$_6$H$_4$-(PMe$_2$)$_2$)$_2$Cl$_2$][BF$_4$]. This difference is a little larger than the expected uncertainty in the EXAFS data, and it may be that the presence of the o-C$_6$F$_4$ backbone and the resulting weaker donor power may have produced slightly longer Fe–P bonds. In the case of the Fe(IV) complex, the EXAFS data distinguished two shells, clearly evident in the very broad and slightly split peak in the Fourier transform (Figure 3).

In all the Fourier transforms a small peak (above noise level) is observed between 4 and 4.5 Å, and this is most probably due to ring carbon atoms. However, these do not correspond to any "real" iron–carbon distances, and may result from multiple-scattering phenomena. They were not therefore used in the fit, and some effect of this can be seen in the EXAFS at low K values where low Z elements at this distance would be most apparent.

A comparison of the Fe–P and Fe–Cl bond lengths in the three title complexes shows that, along the series Fe^{II}–Fe^{III}–Fe^{IV}, the Fe–P bonds lengthen and the Fe–Cl bonds shorten. [Note that in these three complexes *only* the Fe oxidation state changes; the coordinating ligands are identical.] The lengthening of the Fe–P bonds with increasing metal oxidation state probably reflects decreased Fe–P orbital overlap as the metal orbitals contract. Correspondingly, the reverse trend in Fe–Cl bond lengths shows increasing interaction of the σ- and π-donor chlorines with the metal, Fe^{II} < Fe^{III} < Fe^{IV}. Some destabilizing π-repulsion may be present in the Fe(II) complex between the chlorine π-orbitals and the filled (t$_{2g}^6$) metal orbitals.[34] The short Fe–Cl bond length in the Fe(IV) complex correlates well with ^{57}Fe Mössbauer data on the diarsine analogue,[24] which showed a strengthening of the ligand field along the Cl–Fe–Cl axis. It also correlates with the

electronic spectral data (above). This EXAFS study has shown that significant changes in Fe–P and Fe–Cl bond lengths occur with oxidation state changes. It also shows that the technique can yield reliable structural data even for highly unstable complexes, which probably could not be obtained in any other way.

Experimental Section

Physcial measurements were made as described in previous parts of this series. Many of the iron(II) or iron(III) complexes were made by published routes or minor modifications thereof: viz. [Fe(o-C$_6$H$_4$-(PMe$_2$)$_2$)$_2$X$_2$][BF$_4$],[17] [Fe(o-C$_6$H$_4$(AsMe$_2$)$_2$)$_2$X$_2$][BF$_4$],[36] [Fe(o-C$_6$F$_4$-(PMe$_2$)$_2$)$_2$Cl$_2$][BF$_4$],[37] [Fe(cis-Ph$_2$PCH=CHPPh$_2$)$_2$X$_2$],[38] [Fe(2,2'-bpy)$_2$X$_2$],[39] and [Fe(phen)$_2$X$_2$].[40] Other Fe(III) complexes were made by the method described below.

Anhydrous FeX$_3$ (1 mmol) (Alfa Inorganics) was dissolved in absolute ethanol (10 cm^3); the solution was filtered and treated with the ligand (1 mmol) under a dry-nitrogen atmosphere. After 15 min of stirring at room temperature, excess 40% aqueous fluoroboric acid was added, and after a further 1 h, the red or green solids were separated, rinsed with ethanol (2 × 10 cm^3), and dried in vacuo. Anal. Calcd for [Fe(o-C$_6$F$_4$(PMe$_2$)$_2$)$_2$Br$_2$][BF$_4$] (C$_{20}$H$_{24}$BBr$_2$F$_{12}$FeP$_4$): C, 28.5; H, 2.9. Found: C, 28.3; H, 2.9. ν(FeBr) = 300 cm^{-1}. Anal. Calcd for [Fe(o-C$_6$H$_4$-(PMe$_2$)(AsMe$_2$))$_2$Cl$_2$][BF$_4$] (C$_{20}$H$_{32}$As$_2$BCl$_2$F$_4$FeP$_2$): C, 34.4; H, 4.6. Found: C, 34.2; H, 4.5. Calcd for [Fe(o-C$_6$H$_4$(PMe$_2$)(AsMe$_2$))$_2$Br$_2$]-[BF$_4$] (C$_{20}$H$_{32}$As$_2$BBr$_2$F$_4$FeP$_2$): C, 30.5; H, 4.1. Found: C, 30.4; H, 4.0. Calcd for [Fe(Me$_2$PCH$_2$CH$_2$PMe$_2$)$_2$Cl$_2$][BF$_4$] (C$_{12}$H$_{32}$BCl$_2$F$_4$FeP$_4$): C, 28.1; H, 6.3. Found: C, 28.1; H, 6.2. μ_{eff} = 2.21 μ_B. Anal. Calcd for [Fe(Me$_2$PCH$_2$CH$_2$PMe$_2$)$_2$Br$_2$][BF$_4$] (C$_{12}$H$_{32}$BBr$_2$F$_4$FeP$_4$): C, 23.9; H, 5.4. Found: C, 23.6; H, 5.2. ν(FeBr) = 291 cm^{-1}.

[Fe(o-C$_6$H$_4$(PPh$_2$)$_2$)$_2$X$_2$] (X = Cl, Br). FeX$_2$·4H$_2$O (1 mmol) was refluxed in EtOH (15 cm^3) with iron filings and then filtered into a stirred solution of the ligand (2 mmol) in CH$_2$Cl$_2$ (15 cm^3) and EtOH (10 cm^3). The solvent volume was slowly reduced in vacuo at 0 °C. The cream-colored [Fe(o-C$_6$H$_4$(PPh$_2$)$_2$)$_2$X$_2$] products precipitated readily and were filtered off, washed with EtOH (5 cm^3), and dried in vacuo. Anal. Calcd for [Fe(o-C$_6$H$_4$(PPh$_2$)$_2$)$_2$Cl$_2$] (C$_{60}$H$_{48}$Cl$_2$FeP$_4$): C, 70.7; H, 4.7. Found: C, 71.0; H, 4.9 Calcd for [Fe(o-C$_6$H$_4$(PPh$_2$)$_2$)$_2$Br$_2$] (C$_{60}$H$_{48}$Br$_2$FeP$_4$): C, 65.0; H, 4.4. Found: C, 64.8; H, 4.3.

Fe(IV) Complexes. [Fe(o-C$_6$H$_4$(AsMe$_2$)$_2$)$_2$Cl$_2$][BF$_4$]$_2$. [Fe(o-C$_6$H$_4$-(AsMe$_2$)$_2$)$_2$Cl$_2$][BF$_4$] (ca. 0.4 g), finely divided, was cooled to –20 °C and treated with concentrated HNO$_3$ (20 cm^3) that contained a few drops of concentrated HCl. The mixture was rapidly stirred, and after 5 min, during which time the solution darkened, most of the solid had dissolved. The solution was filtered, and HBF$_4$ (45%) was filtered dropwise into the filtrate until precipitation began. A further quantity of HBF$_4$ (8 cm^3) was added. After 5 min at –20 °C, the black-purple precipitate was isolated by filtration, washed with 5% HBF$_4$, and dried in vacuo.

[Fe(o-C$_6$H$_4$(AsMe$_2$)$_2$)$_2$Br$_2$][BF$_4$]$_2$ and [Fe(L-L)$_2$X$_2$][BF$_4$]$_2$ (L-L = o-C$_6$H$_4$(PMe$_2$)(AsMe$_2$), o-C$_6$H$_4$(PMe$_2$)$_2$; X = Br, Cl) were similarly prepared.

[Fe(Me$_2$PCH$_2$CH$_2$PMe$_2$)$_2$Cl$_2$][BF$_4$]$_2$. [Fe(Me$_2$PCH$_2$CH$_2$PMe$_2$)$_2$Cl$_2$][BF$_4$] (ca. 0.3 g) was dissolved in trifluoroacetic acid (10 cm^3). Chlorine gas was bubbled through the mixture until the light mauve solution had become dark mauve. HBF$_4$ (45%) (5 cm^3) was added to

(32) Gurman, S. J.; Binstead, N.; Ross, I. *J. Phys. C* **1984**, *17*, 143.
(33) Cotton, F. A.; Murillo, C. A. *Inorg. Chem.* **1975**, *14*, 2467.
(34) DiVaira, M.; Midollini, S.; Sacconi, L. *Inorg. Chem.* **1981**, *20*, 3430.
(35) Higgins, S. J.; Jewiss, H. C.; Levason, W.; Webster, M. *Acta Crystallogr., Sect. C: Cryst. Struct. Commun.* **1985**, *C41*, 695.

(36) Nyholm, R. S. *J. Chem. Soc.* **1950**, 851.
(37) Higgins, S. J.; Levason, W. *Inorg. Chem.* **1985**, *24*, 1105.
(38) Levason, W.; McAuliffe, C. A.; Khan, M. M.; Nelson, S. M. *J. Chem. Soc., Dalton Trans.* **1976**, 1778.
(39) Basolo, F.; Dwyer, F. P. *J. Am. Chem. Soc.* **1954**, *76*, 1454.
(40) Broomhead, J. A.; Dwyer, F. P. *Aust. J. Chem.* **1961**, *14*, 250.

the mixture, and the solvent was reduced to ca. 2 cm³ by using a vacuum line.

The mixture was placed at -10 °C for 14 h and yielded some mauve/black crystals. These were isolated by filtration, quickly washed with CFCl₃ (4 × 5 cm³) at 0 °C, and dried in vacuo.

All measurements were made on freshly prepared samples. When necessary, samples were stored in sealed tubes at -20 °C in the dark.

EXAFS. EXAFS data at the iron K-edge were recorded at the Daresbury Synchrotron Radiation Source operating at an energy of 2.0 GeV with an average current of 160 mA. Transmission EXAFS data were recorded upon freshly prepared (~24 h old) samples at room temperature, which had been stored at ca. -10 °C in the dark, the samples being placed between "Sellotape" strips. Powdered samples ca. 0.5 mm thick were used, and two or three data sets were recorded upon each sample. No changes in the EXAFS were evident with successive scans, indicating no significant decomposition during the data collection.

Contribution from the Department of Chemistry,
University of Rochester, Rochester, New York 14627

Preparation and Structural Comparison of the Ruthenium(0) Derivatives Ru(DMPE)₂L (L = PMe₃, CO; DMPE = 1,2-Bis(dimethylphosphino)ethane)

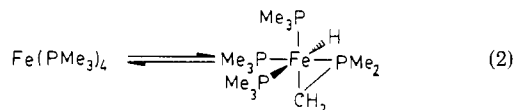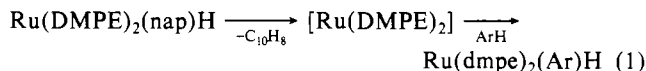William D. Jones*† and Emanuela Libertini

The thermal reaction of Ru(DMPE)₂(nap)H (DMPE = 1,2-bis(dimethylphosphino)ethane; nap = naphthyl) with PMe₃ results in the formation of the new zerovalent derivative Ru(DMPE)₂(PMe₃). The molecule crystallizes in orthorhombic space group *Pnam* with $Z = 4$ ($d_{calcd} = 1.38$ g/cm³) and lattice parameters $a = 16.3540$ (18) Å, $b = 9.3240$ (30) Å, and $c = 16.0210$ (23) Å. The structure displays a square-pyramidal geometry in which the PMe₃ occupies the apical position. Separate modeling of two disorders due to 4-fold rotation of the DMPE ligands about the apical Ru–P vector and 2-fold rotation of the PMe₃ ligand gives refinement to $R_1 = 0.042$, $R_2 = 0.066$. Some reactions of the low-valent derivative are reported. Displacement of PMe₃ by CO occurs at 25 °C, producing Ru(DMPE)₂(CO). Similarly, P(CD₃)₃ exchanges with coordinated PMe₃ more slowly. Neopentyl isocyanide slowly displaces PMe₃ at higher temperatures to give the isocyanide derivative. The CO adduct crystallizes in orthorhombic space group *Pbca* with $Z = 16$ and lattice parameters $a = 19.110$ (9) Å, $b = 23.116$ (6) Å, and $c = 18.780$ (6) Å, the non-hydrogen atoms being refined to $R_1 = 0.048$, $R_2 = 0.066$. A trigonal-bipyramidal geometry is observed in which the CO occupies an equatorial site. The mechanism of substitution indicates both associative and dissociative pathways.

Introduction

The tremendous reactivity of transition-metal complexes in lower oxidation states has resulted in a wide variety of oxidative-addition chemistry of these low-valent metal derivatives.[1] The reducing capability of these metals is found to be affected by the ligands attached to the metal. Good donor ligands such as hydride, η⁵-cyclopentadienyl, and trialkylphosphine are all found to effectively increase the electron density on the metal center, whereas electron-withdrawing ligands such as CO or PF₃ reduce the tendency of the metal to act as a reducing agent.

Both iron(0) and ruthenium(0) complexes are known to be very reactive toward the oxidative addition of C–H bonds.[2-7] Twenty years ago Chatt reported the preparation of Ru(DMPE)₂(nap)H (DMPE = 1,2-bis(dimethylphosphino)ethane; nap = naphthyl) by the reduction of Ru(DMPE)₂Cl₂ with sodium naphthalenide. The former complex was observed to undergo reductive elimination of naphthalene at 60 °C to produce a reactive 16-electron ruthenium(0) intermediate that would react with other aromatic C–H bonds (eq 1).[2] The related iron complex [Fe(PMe₃)₄] was

$$ Ru(DMPE)_2(nap)H \xrightarrow[-C_{10}H_8]{} [Ru(DMPE)_2] \xrightarrow[ArH]{} $$
$$ Ru(dmpe)_2(Ar)H \quad (1) $$

$$ Fe(PMe_3)_4 \rightleftharpoons \quad (2) $$

prepared by both Muetterties[4] and Karsch and Klein[5] and was found to be in equilibrium with the internally metalated species (eq 2). The analogous chemistry with the PMe₃ derivatives of

(1) Halpern, J. *Acc. Chem. Res.* **1970**, *3*, 386-392. Collman, J. P.; Hegedus, L. S. *Principles and Applications of Organotransition Metal Chemistry*; University Science: Mill Valley, CA, 1980.
(2) Chatt, J.; Davidson, J. M. *J. Chem. Soc.* **1965**, 843-855.
(3) Ittel, S. D.; Tolman, C. A.; English, A. D.; Jesson, J. P. *J. Am. Chem. Soc.* **1976**, *98*, 6073-6075. Tolman, C. D.; Ittel, S. D.; English, A. D.; Jesson, J. P. *J. Am. Chem. Soc.* **1979**, *101*, 1742-1751. Ittel, S. D.; Tolman, C. A.; English, A. D.; Jesson, J. P. *J. Am. Chem. Soc.* **1978**, *100*, 7577-7585.
(4) Rathke, J. W.; Muetterties, E. L. *J. Am. Chem. Soc.* **1975**, *97*, 3272-3273.
(5) Karsch, H. H.; Klein, H. F.; Schmidbaur, H. *Chem. Ber.* **1977**, *110*, 2200-2210.
(6) Morris, R. H.; Shiralian, M. *J. Organomet. Chem.* **1984**, *260*, C47-C51.
(7) Werner, H.; Werner, R. *J. Organomet. Chem.* **1981**, *209*, C60-C64. Werner, H.; Gotzig, J. *Organometallics* **1983**, *2*, 547-549.

†A. P. Sloan Fellow, 1984-1986, and Camille and Henry Dreyfus Teacher-Scholar, 1985-1987.